FULL PAPER

$Ti_8O_8(OOCR)_{16}$, a New Family of Titanium–Oxo Clusters: Potential NBUs for Reticular Chemistry

Théo Frot,[a,b] Sébastien Cochet,[c] Guillaume Laurent,[a,b] Capucine Sassoye,[a,b] Michael Popall,[c] Clément Sanchez,[a,b] and Laurence Rozes*[a,b]

The reactions of titanium alkoxides with a large excess of different carboxylic acids under nonhydrolytic conditions leads to the reproducible formation of well-defined nano-building units (NBUs) with the formula $[Ti_8O_8(OOCR)_{16}]$ [R $= C_6H_5$, $C(CH_3)_3$, CH_3]. The structures of these titanium–oxo–carboxylate clusters have been determined by crossing different characterization techniques and methodologies (single-crystal X-ray diffraction, ^{13}C and ^1H NMR spectroscopy, and FTIR spectroscopy). These NBUs are obtained in high yields and, since all the alkoxo ligands have been removed by using solvothermal-synthesis conditions, they present better stability upon hydrolysis than the often reported alkoxo–carboxylate–titanium–oxo clusters $[Ti_n$-$O_{2n-x/2-y/2}(OR')_x(OOCR)_y]$ ($n \geq 2$; $x \geq 1$; $y \geq 1$). In addition, the solubility and transferability of these clusters in common solvents can be tuned by selecting the nature of the organic ligand. Moreover, we also report for the first time, a robust post-modification of the carboxylate ligands by transesterification reactions on the titanium–oxo clusters. These reactions keep the integrity of the octameric titanium–oxo core intact, while completely exchanging the organic shell of the cluster. This family of $[Ti_8O_8(OOCR)_{16}]$ clusters, which present 16 points of extension, a symmetric shape, and the ability to be post-modified with conservation of the core structure, can therefore be considered as interesting NBUs to form new metal–organic frameworks.

Introduction

An extraordinary amount of research has appeared over the last decades in the field of hybrid materials, indicating the growing interest of chemists, physicists, and materials researchers to fully exploit the opportunity of creating innovative materials and devices by taking advantage of the best of the three realms: inorganic, organic, and biological.[1,2] This field of research initially grew out of the sol–gel community,[3–5] and is at present thriving with the appearance of a new class of mesoscopic hybrid structures engineered on the molecular or nanometer scales to satisfy the requirements for a variety of applications from biological and chemical sensing, catalysis, selective separation, to optical communications.[6–9] Among the different strategies used to design nanostructured inorganic–organic hybrids, nano-building block-based (NBBs or NBUs) ones present numerous advantages that have already been em-

phasized in a few feature articles.[10–13] Because of their rich and versatile chemistry, titanium–oxo clusters have been extensively investigated by several research groups[14–18] including the Wien[19–25] and Paris[26–39] groups.

Different approaches are usually applied to create functional building blocks for further hybrid material elaboration. In order to engineer NBU-based hybrid nanocomposites, metal–oxo clusters with functional ligands can be prepared by two strategies. The functional groups can either be introduced during a cluster "one-pot synthesis" or grafted onto a preformed cluster. The first method has been successfully used for the preparation of a variety of carboxylate- or β-diketonate-substituted metal–oxo clusters by reaction of metal alkoxides with carboxylic acids or β-diketones, with concomitant ester (and water) formation resulting in the formation of oxo and hydroxo ligands. One particular advantage of such compounds is that they allow the easy introduction of functional substituents.[10,12] Nevertheless, by this method one has no control over the metal–oxo core structure or the number of the functional ligands. However, the chemical modification of well-defined robust NBUs opens the possibility to a controlled design of the new hybrid architectures. The post-modification method is a less general and more difficult approach to create functional metal–oxo clusters. The reason for this is that the post-synthesis modification requires labile-surface organic groups, and the simultaneous balancing of charges and coordination numbers upon substitution of these groups. Sub-

[a] UPMC Univ Paris 06, UMR 7574, Chimie de la Matière Condensée de Paris, Collège de France,
11 place Marcelin Berthelot, 75005 Paris, France
[b] CNRS, UMR 7574, Chimie de la Matière Condensée de Paris,
75005 Paris, France
Fax: +33-1-44271504
E-mail: laurence.rozes@upmc.fr
[c] Fraunhofer Institut für Silicatforschung (ISC),
Neunerplatz 2, 97082 Würzburg, Germany

stitution can therefore only be expected to proceed, without major difficulties, if both the number of the occupied coordination sites and the charges of the entering ligands are the same as those of the leaving groups.

The post-modification of titanium–alkoxo–oxo clusters has been successfully investigated by using the [Ti$_{16}$O$_{16}$(OEt)$_{32}$] cluster.[33] By alkoxo exchange reactions, building units with polymerizable (styrene or methacrylate) groups and preservation of the [Ti$_{16}$O$_{16}$] oxo core have been isolated and then copolymerized with vinyl monomers in order to form hybrid networks with high mechanical responses.[34,36,40] The post-introduction of complexing multidentate ligands, such as carboxylates, sulfonates, phosphonates, β-diketonates, etc., to bind the organic groups directly to the metal atoms at the surface of the metal–oxo clusters is, in general, more difficult to achieve than trans-alcoholysis. Indeed, [Ti$_{16}$O$_{16}$(OEt)$_{32}$] reacts with carboxylic acids leading to cluster cleavage especially for higher carboxylic acid/Ti ratios.[38] Similarly, the reaction of [Ti$_7$O$_4$(OEt)$_{20}$] with benzoic acid leads to a different cluster, [Ti$_6$O$_4$(OEt)$_{14}$(OOCPh)$_2$], with a major rearrangement of the cluster core, despite the presence of bridging OR groups in the starting cluster.[21] Nevertheless, Schubert et al.[22] have reported that [Ti$_3$O(OiPr)$_{10}$] or [Ti$_3$O(OiPr)$_9$(OMe)] clusters react with benzoic acid, leading quantitatively to [Ti$_3$O(OiPr)$_8$(benzoate)$_2$] with the conservation of the oxo core structure. Because a tridentate ligand is replaced by a bidentate one with the same charge, one of the coordination sites at one of the titanium atoms must be left empty (one titanium atom does indeed change its coordination number from six to five). A higher proportion of benzoic acid leads to a degradation of the [Ti$_3$O(OR)$_{10}$] clusters. Except for this latter example, in general, the structure of titanium–oxo–alkoxo clusters is not preserved upon substitution of alkoxo ligands by carboxylate ones.

The presence of residual alkoxo ligands in carboxylate-substituted oxo clusters [Ti$_n$O$_{2n-x/2-y/2}$(OR')$_x$(OOCR)$_y$] ($n \geq 2$; $x \geq 1$; $y \geq 1$) is also responsible for the low stability of the clusters towards hydrolysis. A possible solution for avoiding the stability problem of clusters against complexing ligands is to synthesize new titanium–oxo clusters that are free from fragile alkoxy groups but already carrying the bidentate ligands.

Reactions between titanium alkoxides and carboxylic acids have been widely studied.[4,41–43]. Depending on the Ti/RCOOH and H$_2$O/Ti ratios, a large set of titania-based materials including stable colloids, monolithic gels, and submicron powders have been described. It is worth mentioning that at room temperature, under nonaqueous conditions, a large excess of acetic acid with the titanium alkoxides results in the formation of a poorly crystalline titanium–oxo acetate of the general formula [TiO(OAc)$_2$].[44] On the basis of these ancient results, the formation of titanium–oxo-based materials by the action of a large excess of carboxylic acid (benzoic, pivalic, and acetic acids) on [Ti(OiPr)$_4$] (RCOOH/Ti = 10:1) under solvothermal conditions is presently being investigated. Solvothermal syntheses, under nonhydrolytic conditions, have shown a huge po-

tential to produce innovative nanomaterials as demonstrated by the work of Niederberger et al.[45,46]

The present work reports the high yield (>95%) and reproducible synthesis of octameric oxo clusters with the formula [Ti$_8$O$_8$(OOCR)$_{16}$] [R = C$_6$H$_5$, C(CH$_3$)$_3$ and CH$_3$]. The resulting compounds, analyzed by X-ray diffraction, consist of a ring of eight [TiO$_6$] octahedra linked by eight μ$_2$-oxo bridges. ^{13}C and ^{1}H NMR spectroscopic measurements enable us to clearly distinguish between the two crystallographically different carboxylate ligands bonded to the titanium atom in the axial and equatorial positions. Because all of the alkoxo ligands have been removed, the stability of these new NBUs towards hydrolysis and complexing ligands is considerably increased. Indeed, we report for the first time, the ability of the titanium–oxo–carboxylate clusters to be post-modified by transesterification reactions with the preservation of the metal–oxo core. The post-modification by bidentate ligands on Ti$_8$O$_8$-based titanium–oxo clusters is reported in this paper with the usual molecules such as benzoic, pivalic, and acetic acids. The present carboxylate octameric oxo clusters [Ti$_8$O$_8$-(OOCR)$_{16}$] appear to be good candidates for further hybrid-material building.

Results and Discussion

1. Elaboration of [Ti$_8$O$_8$(OOCR)$_{16}$] Oxo Clusters

The cluster [Ti$_8$O$_8$(OOCC$_6$H$_5$)$_{16}$]·(CH$_3$CN)$_2$·H$_2$O (**Ti$_8$Ph**) is obtained upon reaction of [Ti(OiPr)$_4$] with a large excess of benzoic acid (10:1) in acetonitrile. Yellow crystalline needles are obtained at 100 °C in a closed vessel after 15 h and were analyzed by single-crystal X-ray diffraction techniques (Table 2).

The cluster can be described as an eight-membered-ring vertex of shared TiO$_6$ octahedra, with 16 bridging bidentate benzoate groups pointing outwards (Figure 1a–c). Eight equatorial benzoate groups point up and down alternatively from the plane delimited by the [Ti$_8$O$_8$] ring at a 25° angle, whereas the eight other axial benzoate groups stand up and down perpendicularly. Disorder is observed at the axial groups: two positions per axial phenyl ring have been localized in a ratio of 50:50 (Figure 1a). The global structure can be described as a body-centered tetragonal packing of [Ti$_8$O$_8$] rings where the centered ring is inversed (Figure 1a). The smallest aperture of the ring, measured between the μ$_2$-oxygen atoms, is 6.9561(9) Å. The TiO$_6$ octahedra are slightly contracted towards the μ$_2$-oxygen [<Ti–O$_{(C)}$> 2.0539(3), <Ti–μ$_2$-O> 1.8264(2) Å]. Two molecules of acetonitrile are observed inside the free space delimited by the axial benzoate ligands, and one water molecule is trapped in the middle of the [Ti$_8$O$_8$] ring. Because of the high amount of phenyl groups present in the cluster, there is a possibility of π–π stacking that could be responsible for the cohesion and stability of the structure. However, despite a carefully detailed study of the structure, no such interaction has been found.
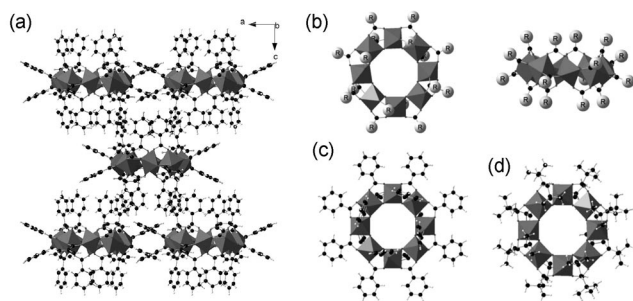
Figure 1. (a) Polyhedral representation of the pseudo-tetragonal C packing of $[Ti_8O_8(OOCC_6H_5)_{16}]\cdot(HOOCC_6H_5)_2\cdot H_2O$ along the *b* axis. (b) Schematic view of the $[Ti_8O_8(OOCR)_{16}]$ ring. (c) and (d) Ti_8O_8 ring for R = C_6H_5 and R = $C(CH_3)_3$, respectively. For $[Ti_8O_8(OOCC_6H_5)_{16}]\cdot(HOOCC_6H_5)_2\cdot H_2O$, because of the *P4* symmetry, four oxygen positions are observed for the free benzoic acid, among which two have to be chosen. The choice has been made to place the oxygen atoms in the same plane as the phenyl ring, which allows for better electronic delocalization.

The reaction of an excess of pivalic acid (10:1) with $Ti(OiPr)_4$, carried out under the same conditions (acetonitrile at 100 °C for 15 h), leads to the formation of white crystals. Redissolution into THF and further recrystallization leads to a higher crystal quality, which enables the resolution of the $[Ti_8O_8\{OOCC(CH_3)_3\}_{16}]\cdot(C_4H_8O)_2$ (**Ti₈*t*Bu**) structure from single-crystal X-ray diffraction (Table 2). The crystal structure of the oxo core of $[Ti_8O_8\{OOCC(CH_3)_3\}_{16}]$ is identical to the one of **Ti₈Ph**, with 16 pivalato ligands surrounding the Ti_8O_8 ring (Figure 1d). Two THF molecules per cluster are localized; no water molecule has been found at the center of the ring in this case.

The carboxylate-substituted titanium–alkoxo clusters constitute an important subclass of titanium–oxo clusters whose nuclearity varies from two $[Ti_2O(OiPr)_2(HOiPr)_2(OOC–CCl_3)_4]$[47] to nine $[Ti_9O_8(OR)_4(OOCR')_{16}]$.[23] In these structures, the degree of condensation is limited by the increased coordination requirement of the carboxylate ligands that are always bridging {exception for chlorocarboxylates in $[Ti_2O(OiPr)_2(HOiPr)_2(OOCCCl_3)_4]$[47] with terminal carboxylates}. In all carboxylate-substituted titanium–oxo clusters, the Ti centers are sixfold coordinated with only one exception {one Ti atom in $[Ti_3O(OR)_8(OOCR')_2]$[22,48] is fivefold coordinated}. The carboxylate/titanium ratio (*z*) must be lower than two to accommodate the OR ligands. The maximum value of *z* was found in a crystalline derivative of composition $[Ti_9O_8(Pr)_4\{OOCC(CH_3)=CH_2\}_{16}]$.[23] This compound was obtained by treating $[Ti(OPr)_4]$ with a fourfold excess of methacrylic acid at ambient temperature. The water responsible for the hydrolysis of the OPr group was generated in situ by esterification of free methacrylic acid with cleaved alcohol. The compound consists of a ring of nine $[TiO_6]$ octahedra linked by six μ_2- and two μ_3-oxo bridges. All titanium atoms are octahedrally coordinated, and all carboxylate groups are bridging. The higher degree of substitution by the bidentate

carboxylate ligands forces the structure to become less condensed, since a coordination number larger than six is not possible. A smaller degree of substitution was found in $[Ti_6O_4(OR)_8(OOCR')_8]$,[19,49] $[Ti_6O_4(OR)_{12}(OOCR')_4]$,[27] and $[Ti_4O_4(OR)_4(OOCR')_4]$.[50] The titanium atoms are octahedrally coordinated in all derivatives, and the carboxylate ligands are bridging. The linkage between the octahedra shows variations; the main difference between the cluster types is the ratio between shared vertices and edges. The titanium atoms are connected by μ_2-oxo and μ_3-oxo bridges {μ_4-oxo in $[Ti_4O_2(OiPr)_{10}(OOCR)_2]$[15,51]}. The presence of at least one μ_3-oxo bridge in these structures enables most of the carboxylate-substituted Ti–oxo clusters to be described as substructures of the cubic $[Ti_4O_4]$ motif.[24] Because the maximum coordination number of titanium is restricted to six, the expected maximum carboxylate/titanium ratio of oxo–titanium carboxylates is 2, i.e. the composition $[TiO(OOCR)_2]$ (provided that all the carboxylate ligands are bidentate and the $[TiO_6]$ octahedra are linked by μ_2-oxo bridges). We demonstrate the possibility of obtaining well-defined nanoobjects (Ti_8O_8 clusters), contrary to previously reported results, which describe the formation of titanium–oxo carboxylate polymers with fully released alkoxo ligands.[44] However, such a $[Ti_8O_8]$ ring has already been reported $\{[Ti_8O_8(O_2CC_6F_5)_{16}]\cdot(C_6H_5-CH_3)_n\}$ with a lower symmetry ($P\bar{1}$). It has been prepared from a more reactive precursor ($TiCl_4$) and stronger acids (such as pentafluorobenzoic acid, $C_6F_5CO_2H$). Two free toluene molecules were trapped inside the remaining space between the axial fluorophenyl rings.[52] The same octameric structure was also obtained from titanium alkoxides and three different carboxylic acids [$tBuCO_2H$, $tBuCH_2-CO_2H$, or $Et(CH_3)_2CCO_2H$]. These oxo clusters, obtained in lower yield, have been described as weakly stable species.[53]

The experimental conditions have been optimized in order to obtain stable, pure carboxylate clusters with high yields. Indeed, the heating of a solution of titanium(IV) isopropoxide, $[Ti(OiPr)_4]$, with an excess of benzoic acid (10:1) in acetonitrile at 80 °C over 2 d leads to a precipitated powder with very low crystallinity. The XRD pattern shows only a few very broad peaks that cannot be associated with any known phase (see Supporting Information). The FTIR spectrum shows the presence of unreacted benzoic acid (νCOO_{as} = 1692 cm^{-1}; νCOO_s = 1294 cm^{-1}; $\Delta\nu$ = 400 cm^{-1}), and strong vibrations can be attributed to bidentate benzoate groups (νCOO_{as} = 1514 cm^{-1} and νCOO_s = 1398 cm^{-1}; $\Delta\nu$ = 116 cm^{-1}). Isopropoxy groups are detected by the $\nu C-H$ (between 2970 and 2850 cm^{-1}) and $\nu Ti-O-C$ (1010 cm^{-1}) vibrations (see Supporting Information). The bands below 720 cm^{-1} are attributed to the Ti–O vibrations. The ^{13}C MAS solid-state NMR spectrum confirms the presence of some titanium-bonded benzoate groups [δ = 175.8 ($OOCC_6H_5$) and 130.9 ($OOCC_6H_5$) ppm], a small amount of unreacted benzoic acid [δ = 172.0 ($HOOCC_6H_5$) ppm, and some isopropoxide groups {δ = 86.3 [$OCH(CH_3)_2$], 24.5 [$OCH(CH_3)_2$] ppm}. Quantitative NMR spectroscopic measurements enable the ratio of 1 isopropoxy group to 4.2

benzoate groups to be calculated from the integration of the peaks at δ = 130.9 (aromatic C atoms) and 24.5 (methyl groups of isopropyl group) ppm (see Supporting Information). This leads to the proposed [TiO(C$_6$H$_5$COO)$_{1.6}$-(OiPr)$_{0.4}$] formula. In the present work, the clusters show a high stability towards nucleophilic species, especially towards water. The samples can be manipulated without any precaution, the structure of the compounds (determined by XRD or NMR spectroscopy) are still unchanged after a few weeks in a moist atmosphere.

It can be stressed that the same solution leads to both the amorphous [TiO(C$_6$H$_5$COO)$_{1.6}$(OiPr)$_{0.4}$] phase and the oxo cluster **Ti$_8$Ph**, depending on the progress of the reaction (temperature and time of synthesis: 100 °C for 15 h for **Ti$_8$Ph**; 80 °C for 2 d for the amorphous phase). In order to have a better understanding of the evolution of [TiO(C$_6$H$_5$COO)$_{1.6}$(OiPr)$_{0.4}$] over **Ti$_8$Ph**, SEM pictures of powders prepared under different conditions have been taken (Figure 2). For the sample heated at 80 °C for 2 d, with a carboxylic acid/titanium ratio of 5:1 or 10:1, Figure 2a–d mainly shows well-defined spheres of approximately 2–5 µm. These spheres may grow and aggregate themselves to form some larger entities of several tenths of a micrometer in length. Each observed sample shows all these characteristics: small or larger spheres that can be more or less aggregated. Variation of the heating time between 1 and 2 d does not seem to affect either the crystallinity or the morphology of the powder; only the yield. Still, for 2 d at 80 °C for a benzoic acid/Ti ratio of 20:1 the spheres tend to aggregate and merge into parallelepiped blocs of hundreds of micrometers in length (Figure 2e–f). Here the crystallinity of the sample remains very low. For 2.5 d (80 °C, benzoic acid/titanium, 10:1), we still observe some small spheres; probably the amorphous phase, but there is mainly the presence of the well-defined needles that are characteristic of the **Ti$_8$Ph** phase (Figure 2g–i). Synthesis at a higher temperature leads to larger crystals (Figure 2j). The unstable phase with residual alkoxo ligands can thus be seen as an amorphous intermediate of the crystalline and stable **Ti$_8$Ph**. The synthesis conditions allow the complete substitution of the remaining alkoxide groups by the carboxylate ligands, leading to a well-defined stable entity. From a large excess of carboxylic acid (even with weak acids), the formation of pure oxo–carboxylate clusters is achieved under solvothermal conditions.

In parallel with the X-ray diffraction determination, NMR measurements have been performed on the [Ti$_8$O$_8$(OOCR)$_{16}$] oxo clusters. For the ^{13}C MAS solid-state NMR spectrum of **Ti$_8$Ph**, two groups of peaks are clearly observed (Figure 3): one group of two peaks at δ = 175.7 and 176.9 ppm and one group at δ ≈ 130 ppm. The two crystallographically different carboxylate ligands (axial and equatorial) bonded to the titanium atom, characterized by a difference in the C–O bond lengths, can be differentiated in the solid-state NMR spectrum by the presence of two distinct peaks at δ = 176.9 and 175.7 ppm. The shifts, compared to those of pure benzoic acid expected at δ = 172 ppm, are in agreement with the bridging behavior
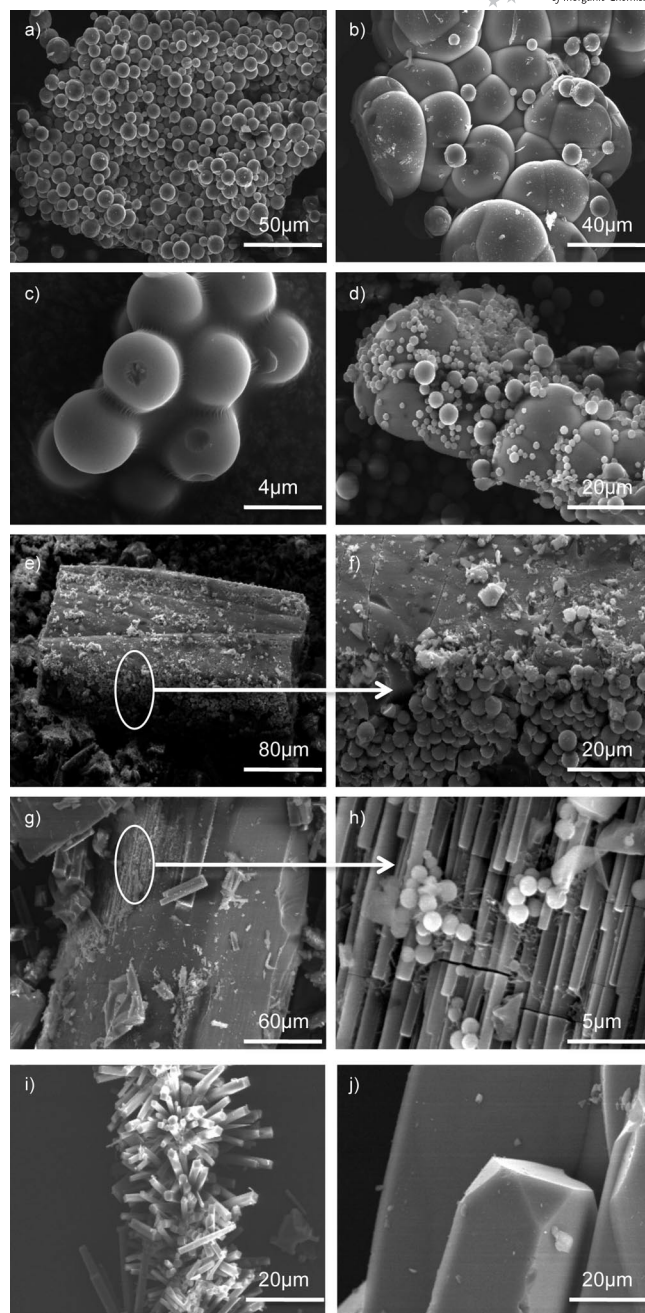

Figure 2. SEM pictures of the amorphous phase [TiO(C$_6$H$_5$COO)$_{1.6}$(OiPr)$_{0.4}$] and crystalline needles [Ti$_8$O$_8$(OOCC$_6$H$_5$)$_{16}$]. The samples are prepared with the following experimental parameters: temperature [°C]/time [d]/Ti:benzoic ratio: (a–c) 80/2/1:5, (d) 80/2/1:10, (e–f) 80/2/1:20, (g–i) 80/2.5/1:10, (j) 105/2/1:10.

of the carboxylate ligands on the titanium sites. The integrations of the two carboxylate peaks give a ratio of 52.5:47.5.

The crystallographic data show that the axial groups are disordered (two positions in a ratio of 50:50), whereas the equatorial ones are fully defined at a single position. The examination of the calculated isotropic thermal agitation parameter (U_{eq}), associated with the NMR spectroscopic data, allows the assignment of the axial and equatorial carboxylate chemical shifts. Three NMR experiments have
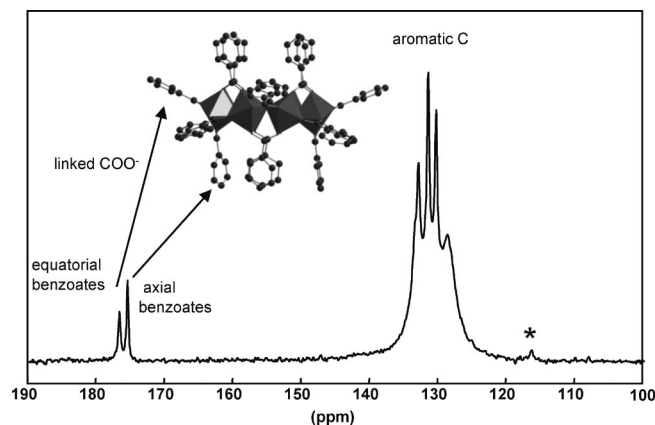
Figure 3. High-power ^{1}H-decoupling ^{13}C MAS NMR (75.47 MHz) spectrum of the [Ti$_8$O$_8$(OOCC$_6$H$_5$)$_{16}$] oxo cluster. *: free acetonitrile.

been done to determine the two carboxylate signals (the axial and the equatorial group): a study of the peak width, a study of the transverse relaxation time T_2' by using variable-delay Hahn echoes, and time obtained by inversion recovery cross polarization (IRCP) analysis, T_{IRCP}. An increase in the mobility causes a thinning of the peak width and a rising of the T_2' and T_{IRCP} time:

$$U_{eq} \propto \text{mobility} \propto T_2^* \propto T_2' \propto T_{IRCP} \propto \frac{1}{\text{width}}$$

The results extracted from the NMR spectroscopic data can be correlated with the ones obtained from the crystallographic measurements (Table 1). Indeed, the resulting longer relaxation time associated with the more mobile species can be associated with the higher calculated isotropic thermal agitation parameter, U_{eq}, obtained by X-ray diffraction. These results allow us to assign the peak at $\delta = 175.4$ ppm to the carbon atoms of the carboxylate axial groups, which are characterized by a higher mobility than the equatorial ones. The peak at $\delta = 176.9$ ppm is then attributed to the carbon atoms of the equatorial benzoate groups.

Table 1. Results extracted from the NMR measurements correlated with those obtained from the crystallographic measurements for the [Ti$_8$O$_8$(OOCC$_6$H$_5$)$_{16}$] cluster.

δ [ppm]	Width [Hz]	T_2^* [ms]	T_2' [ms]	T_{IRCP} [ms]	U_{eq} ($\times 10^3$) [Å^2]
176.9	60.4	5.3	26	0.75	32
175.7	37.7	8.4	46	0.93	43

The peaks centered at $\delta = 130$ ppm are from the aromatic carbon atoms of the benzoato ligands, in the axial or equatorial position. Four peaks can clearly be identified at $\delta = 133.6$, 133.1, 131.6, and 130.5 ppm, but no attribution has been done because of the overlapping of the signals of the axial and equatorial groups.

The additional peaks at $\delta = 116.5$ and -0.4 ppm are attributed to acetonitrile trapped between the axial phenyl groups. The methyl carbon atom is significantly shielded in comparison to the one in free acetonitrile ($\delta = 2.2$ ppm),

whereas the value of the cyano carbon peak remains unchanged ($\delta = 116.9$ ppm). The shift is probably a result of the proximity of the aromatic rings. A similar phenomenon is observed with solvents trapped in arenes.[54,55] Since the trapped nitrile function stands further away from the pocket formed by the benzoate rings, there is no shift in its carbon signals.

The high solubility in common solvents, such as aromatic or halogenated solvents, of the cluster **Ti$_8$tBu** allows to perform liquid-state NMR measurements (Figure 4). By analogy with the results obtained from solid-state NMR spectroscopic studies performed on the **Ti$_8$Ph** cluster, the more deshielded signals are attributed to the atoms in the equatorial position of the structure. In the ^{1}H NMR spectrum, the signal corresponding to the axial ligands is at $\delta = 1.15$ ppm and the one corresponding to the equatorial *tert*-butyl groups is at $\delta = 1.16$ ppm. In the ^{13}C NMR spectrum, the three signals corresponding to the equatorial pivalato ligands [(CH$_3$)$_3$C*C*OO at $\delta = 189.2$ ppm, (CH$_3$)$_3$*C*COO at $\delta = 39.6$ ppm, (*C*H$_3$)$_3$CCOO at $\delta = 27.5$ ppm] are also shielded compared to those of the axial ligands [(CH$_3$)$_3$C*C*OO at $\delta = 187.7$ ppm, (CH$_3$)$_3$*C*COO at $\delta = 39.4$ ppm, (*C*H$_3$)$_3$CCOO at $\delta = 27.3$ ppm].
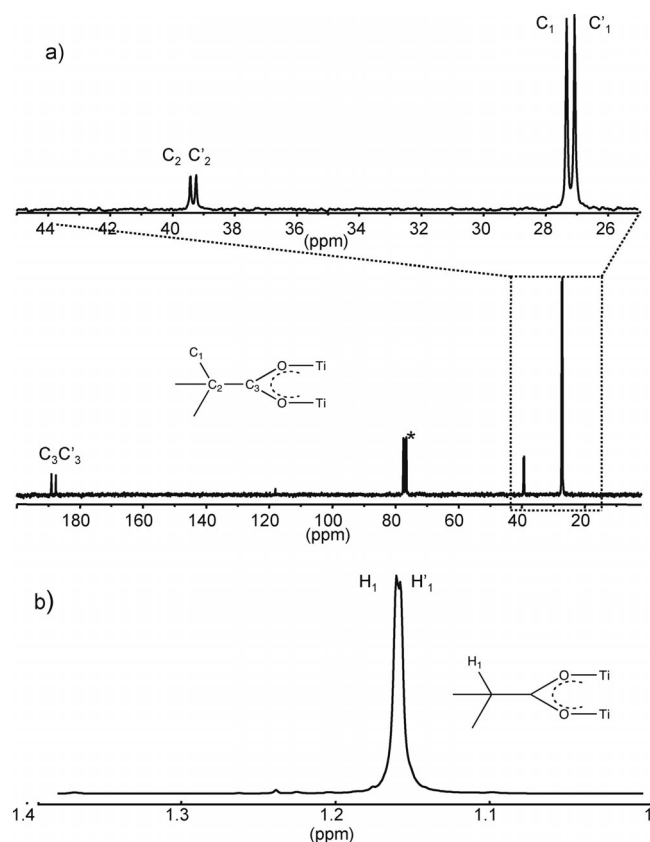
Figure 4. (a) ^{13}C (75.47 MHz) and (b) ^{1}H (300 MHz) liquid-state NMR spectra of [Ti$_8$O$_8$(OOCtBu)$_{16}$]·(C$_4$H$_8$O$_2$)$_2$. *: CDCl$_3$.

The oxo cluster **Ti$_8$Ph** with free benzoic acid located in the crystalline matrix, i.e. a structure formula of [Ti$_8$O$_8$(OOCC$_6$H$_5$)$_{16}$]·(HOOCC$_6$H$_5$)$_2$·H$_2$O, has also been isolated and characterized. In the solid-state ^{13}C NMR

spectrum (Figure 5c), a single sharp peak at $\delta = 165.9$ ppm is attributed to the carboxylic group of the "free" benzoic acid located in the crystals. The difference in the chemical shift to pure benzoic acid ($\delta = 172$ ppm) reflects the specific environment of the molecule trapped inside the cluster. Two causes may be responsible for the chemical shift. The first one is the formation of hydrogen bonds with the water molecule entrapped at the center of the [Ti$_8$O$_8$] ring [O$_w$···O$_{COOH}$ 2.7699(5) Å]. The other reason is the anisotropic aromatic shielding effect analogous to the one observed previously with acetonitrile, since the entrapped free benzoic acid is in the shielding region of four axial aromatic groups. As for the cyano function of acetonitrile in [Ti$_8$O$_8$(OOCC$_6$H$_5$)$_{16}$]·(CH$_3$CN)$_2$ (Figure 5a), there is no shift in the aromatic carbon signals: the trapped aromatic ring stands further away from the pocket formed by the benzoate rings. We have attempted to exchange the free benzoic acid trapped in the oxo cluster with different organic molecules, such as diethyl ether. For the ^{13}C NMR spectrum of the resulting powder (Figure 5b), two peaks at $\delta = 14.8$ and 64.6 ppm corresponding to the carbon atoms of diethyl ether are observed. The chemical shifts are here once again lower than those of free diethyl ether ($\delta = 15.35$ and 65.97 ppm), which confirms that diethyl ether is probably also trapped inside the [Ti$_8$O$_8$] ring. Given the fact that the crystallographic data shows two acetonitrile and two free benzoic acid molecules per [Ti$_8$O$_8$] ring, we can propose that such behavior is also the case with the diethyl ether. The molecular formula should then be [Ti$_8$O$_8$(OOCC$_6$H$_5$)$_{16}$]·(C$_2$H$_5$OC$_2$H$_5$)$_2$·H$_2$O. Moreover, given the fact that the methyl groups are less shielded than the methylene one, we can guess that the oxygen atom of the diethyl ether is pointing directly towards the trapped water molecule. This result emphasizes the possible accessibility of organic mole-

cules inside the cavity generated by the cluster structure and their perfect localization without destruction of the host entity.

2. Chemical Modification of the Carboxylate Ligands of the Octameric Ring Structure

The first approach, which consists of obtaining the [Ti$_8$O$_8$(OOCR)$_{16}$] cluster from the alkoxide, Ti(OiPr)$_4$, and a large excess of acetic acid (1:10), was performed in acetonitrile at 100 °C for 5 d and led to the formation of a crystalline powder. Nevertheless, a single-crystal X-ray diffraction analysis cannot be performed because of the poor quality of the obtained crystals. The presence of bidentate acetato ligands in the coordination shell of the titanium atom is shown by FTIR spectroscopy {characteristic vibrations at 1456 [v_s(COO)] and 1552 [v_{as}(COO)] cm^{-1}}. The simplicity of the solid-state ^{13}C NMR spectrum (Figure 6a) and the high resolution of the peaks suggest the formation of well-defined entities. The similarities between the ^{13}C NMR spectrum of the **Ti$_8$Ph** oxo cluster and the product obtained with acetic acid tends to prove that the same [Ti$_8$O$_8$] core has been obtained. Especially, the peaks at $\delta = 182.5$ and 184.6 ppm suggest that two crystallographically different carboxylate groups are present in a cluster structure. The chemical analyses are in agreement with the formation of an octameric cluster [Ti$_8$O$_8$(OOCCH$_3$)$_{16}$] (**Ti$_8$Me**).
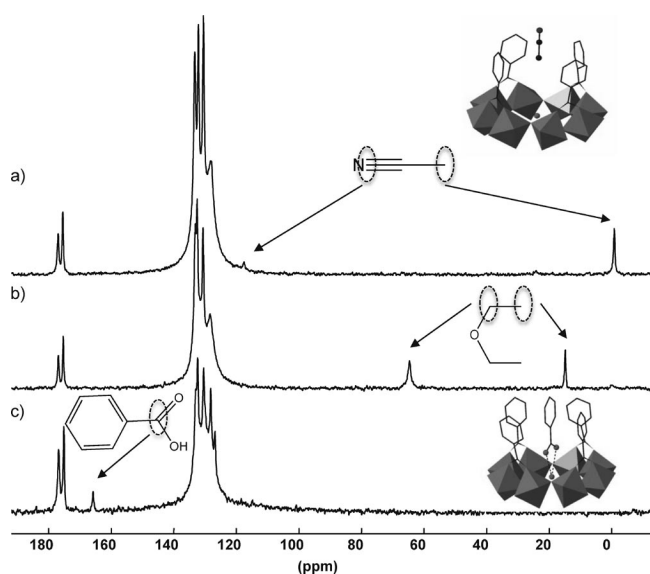

Figure 6. High-power ^{1}H-decoupling ^{13}C MAS NMR (75.47 MHz) spectra of (a) [Ti$_8$O$_8$(OOCCH$_3$)$_{16}$] obtained from [Ti(OiPr)$_4$], (b) [Ti$_8$O$_8$(OOCCH$_3$)$_{16}$] obtained from exchange reactions with [Ti$_8$O$_8$(OOCPh)$_{16}$], (c) intermediate product, and (d) [Ti$_8$O$_8$-(OOCPh)$_{16}$] obtained from [Ti(OiPr)$_4$].

Figure 5. ^{13}C CPMAS NMR spectra and representation of the corresponding pocket of (a) [Ti$_8$O$_8$(OOCC$_6$H$_5$)$_{16}$]·(CH$_3$CN)$_2$·H$_2$O, (b) [Ti$_8$O$_8$(OOCC$_6$H$_5$)$_{16}$]·(C$_2$H$_5$OC$_2$H$_5$)$_2$·H$_2$O, and (c) [Ti$_8$O$_8$(OOCC$_6$-H$_5$)$_{16}$]·(HOOCC$_6$H$_5$)$_2$·H$_2$O.

A second approach has also been investigated, which consists of two consecutive exchanges of the benzoic ligands on the preformed **Ti$_8$Ph** cluster by acetato ligands. Acetic acid (160 equiv.) was added to a yellow dispersion of **Ti$_8$Ph** in acetonitrile (10 acetic acid molecules for 1 benzoate group). The dispersion was heated at reflux for 2 d and then dried under vacuum and washed with acetonitrile, leading to a white powder. This intermediate product was dispersed twice in acetonitrile, and the same quantity of acetic acid was added and the mixture was heated at reflux.

The intermediate product is amorphous. The ^{13}C NMR spectrum clearly shows the partial disappearance of the characteristic signals of benzoato ligands ($\delta = 175.3$ ppm and peaks of aromatic carbon atoms centered at $\delta = 130$ ppm) with the concomitant appearance of two distinguished peaks more deshielded at $\delta = 184.8$ and 182.2 ppm and a single peak at a lower chemical shift ($\delta = 22.7$ ppm) attributed to the methyl group of the acetates (Figure 6c). The second treatment of the amorphous powder leads to the total disappearance of the characteristic benzoate peaks, and only acetate characteristic peaks are observed (Figure 6b). The spectrum can be superimposed with the spectrum obtained for the supposed octameric ring with 16 acetate points of extension. The powder diagram obtained by X-ray diffraction on the fully exchanged cluster is also perfectly superimposable with the one recorded of the acetate cluster built under one-pot conditions from [Ti(OiPr)$_4$]. The peaks at $\delta = 21.1$ and 23.2 ppm are attributed to the CH_3 group of acetate linked to the titanium atom and to the methyl group of free acetic acid, respectively. By analogy with the discussion done on the NMR spectroscopic results on **Ti$_8$Ph**, the most deshielded signal at $\delta = 184.8$ ppm is attributed to equatorial acetate groups, and the signal at $\delta = 182.2$ ppm is attributed to the axial acetate groups. The presence of trapped acetic acid in the structure is also determined by the existence of a peak at $\delta = 174.9$ ppm. The suggested formula is [Ti$_8$O$_8$(OOCCH$_3$)$_{16}$]·(HOOCCH$_3$)$_2$. The reversibility of the transesterification reaction is also demonstrated. Indeed, benzoic acid with **Ti$_8$Me** clusters leads to the formation of **Ti$_8$Ph**; the X-ray pattern of the compounds obtained by an exchange reaction on the preformed cluster is perfectly superimposable with the one recorded for the compound obtained by the "one-pot" synthesis from Ti(OiPr)$_4$ (Figure 7).

The post-modification by transesterification of **Ti$_8$Ph** has also been performed with an excess of pivalic acid in xylene. A change of color from yellow to white after the treatment with pivalic acid is observed. The X-ray diffraction study of the recrystallized white powder and the spectroscopic analysis by ^1H and ^{13}C NMR spectroscopy demonstrate that the resulting compound is **Ti$_8$$t$Bu**. It can be noticed that the opposite reaction (modification of the pivalate group by benzoate) has also been successfully performed.

Despite the strong power of complexation of the carboxylate ligands in a bidentate coordination mode in the coordination sphere of transition-metal centers, the equilibrium reaction can be advantageously displaced towards the formation of the fully substituted octameric cluster, while
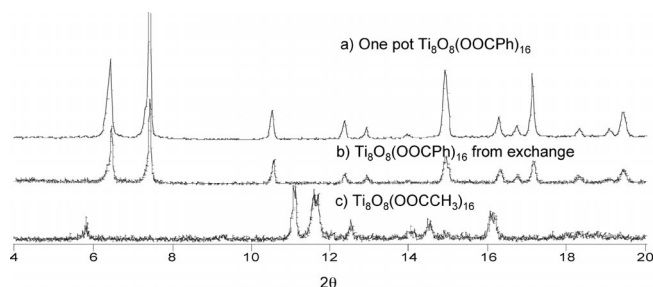

Figure 7. Powder XRD of (a) [Ti$_8$O$_8$(OOCPh)$_{16}$] from the one-pot synthesis; (b) [Ti$_8$O$_8$(OOCPh)$_{16}$] from exchange reactions; (c) [Ti$_8$O$_8$(OOCCH$_3$)$_{16}$] from one-pot synthesis or by transesterification reaction with [Ti$_8$O$_8$(OOCPh)$_{16}$].

maintaining an intact [Ti$_8$O$_8$] oxo core. The reaction proceeds by the formation of an amorphous product, which bears both the entering ligand and the leaving one. A second-step exchange at reflux or under solvothermal conditions allows the formation of the well-defined [Ti$_8$O$_8$] oxo cluster. At this stage of the study we cannot say whether the reaction proceeds at the surface of the octameric oxo core by an exchange of the carboxylate ligands done step by step. However, we cannot exclude the fact that the presence of an excess of free carboxylic acid leads to the destruction (or partial destruction) of the structure to form discreet sub-units, which will further recondense to form a thermodynamically stable complex with the same structure.

Conclusions

Reproducible titanium–oxo–carboxylate clusters have been synthesized with benzoic, pivalic, and acetic acids from titanium alkoxides in high yields. These clusters are constituted by an octameric oxo core surrounded by 16 carboxylate ligands. The solvothermal-synthesis conditions enable the release of all the alkoxy groups (even with weak carboxylic acids) leading to stable NBUs towards nucleophilic reactants. We demonstrate for the first time the ability of these nanoobjects to be post-modified by other organic acids with the preservation of the octameric oxo core allowing the tuning of their solubility and transferability. This post-modification approach should then be further advantageously investigated in the presence of polyfunctional ligands in order to modify the surface connectivity of the nano-building units for hybrid material elaboration. Indeed, the symmetric design of the octameric oxo core and the important number of exchangeable monofunctional ligands allows us to consider these new compounds as appropriate secondary building units for the elaboration of well-defined hybrid structures such as metal–organic frameworks[56–60] that are known to present interesting properties and potential applications in gas storage, separation, catalysis, thin films, magnetism, or drug delivery.[61–63]

Experimental Section

General Methods and Materials: Solid-state NMR experiments were performed with a Bruker AVANCE 300 spectrometer at $B_0 =$

7.04 T with v_0(^{13}C) = 75.47 MHz by using a 4 mm Bruker MAS probe. Samples were spun at the magic angle at 14 kHz by using ZrO$_2$ rotors. ^{13}C MAS NMR spectra were acquired by using a 90° pulse of 4.3 µs and a recycle delay of 30 s with TPPM15 decoupling only during acquisition.[65] The ^{13}C CPMAS experiments were performed with v_{1C} = 64 kHz during the 1 ms contact time and v_{1H} = 50 kHz for ^{1}H 90° pulse, the contact time and the TPPM15 decoupling only during acquisition. The ^{13}C T_2 measurement was achieved by using a 2 ms CP followed by a rotor-synchronized decoupled Hahn echo, with delays ranging from 0.14 to 14.3 ms. The ^{13}C IRCP consists of a 2 ms CP followed by a phase-inversion time ranging from 1 to 500 µs. ^{1}H and ^{13}C liquid NMR experiments were performed with a Bruker AC300 spectrometer (300.13 and 75.47 MHz for ^{1}H and ^{13}C NMR, respectively). [D$_8$]THF was used as the solvent and internal lock. ^{1}H and ^{13}C NMR data are quoted relative to TMS by using the solvent or its protonated impurities as the secondary internal reference (^{1}H NMR: δ = 1.84 and 3.73 ppm; ^{13}C NMR: δ = 25.77 and 68.00 ppm).[66] X-ray diffraction powder patterns were obtained with a Bruker D8 diffractometer (q-2q Bragg–Brentano geometry) operating with Cu-K_α radiation (λ = 1.5418 Å) and equipped with a graphite back monochromator. FTIR spectra were recorded with a Nicolet Magna 550 FTIR spectrometer by using KBr pellets. Thermal properties were measured by thermogravimetric analysis (TGA) under air flux at a heating rate of 2 °C min^{-1} with an SDT 2960 thermal analyzer (TA Instruments). SEM analyses were performed with a Hitachi S-800 field emission scanning electron microscope. High voltage (6–25 kV) and a secondary electron detector were used.

Synthesis of Titanium–Oxo–Carboxylate Cluster [Ti$_8$O$_8$-(OOCC$_6$H$_5$)$_{16}$]·(CH$_3$CN)$_2$·H$_2$O (Ti$_8$Ph): Benzoic acid (5.67 g, 46 mmol) dissolved in acetonitrile (40 g, 970 mmol) was added dropwise to a solution of titanium(IV) isopropoxide (1.5 g, 5.3 mmol) in acetonitrile (8 g, 195 mmol). After a few minutes of stirring, the 100 mL Pyrex autoclave was closed and placed in an oven. The limpid solution was heated at 100 °C for 15 h. Needles appeared at the bottom of the flask. The solvent was removed, and the pale yellow needles (1.71 g, yield 99%) were dried under argon. ^{13}C MAS solid-state NMR: δ = 176.9 and 175.7 (OOCC$_6$H$_5$), 130 (w, OOCC$_6$H$_5$) ppm. TGA: 20–250 °C (4.5 wt.-% loss), 250–390 °C (36 wt.-% loss), 390–480 °C (33.5 wt.-% loss). Selected IR data: $\tilde{v}$ = 3090 (w), 3063 (w), 3030 (w), 2977 (w), 1719 (w), 1693 (m), 1515 (m), 1592 (s), 1535 (m), 1492 (m), 1417 (s), 1176 (m), 1025 (m), 745 (m), 716 (s), 671 (s), 518 (m), 480 (m) cm^{-1}. C$_{14.5}$H$_{11}$N$_{0.25}$O$_{5.13}$Ti (318.6): calcd. C 54.7, H 3.5, N 1.1, Ti 15.0; found C 54.1, H 3.7, N 1.0, Ti 15.2.

Synthesis of Titanium–Oxo–Carboxylate Clusters [Ti$_8$O$_8$-{OOC(CH$_3$)$_3$}$_{16}$]·(C$_5$H$_8$O)$_2$ (Ti$_8$tBu): Pivalic acid (17.5 g, 170 mmol) dissolved in acetonitrile (40 g, 970 mmol) was added dropwise to a solution of titanium(IV) isopropoxide (5 g, 17 mmol) in acetonitrile (8 g, 195 mmol). After a few minutes of stirring, the 100 mL Pyrex autoclave was closed and placed in an oven heated at 100 °C for 3 d. White translucent crystals appeared at the bottom of the flask. The solvent was removed, and the white crystals (4.19 g, yield 94%) were dried under argon. Redissolution in THF and further recrystallization led to higher quality crystals, which enabled an X-ray diffraction structure to be obtained. ^{13}C liquid NMR in CDCl$_3$: δ = 189.2 and 187.7 [OOCC(CH$_3$)$_3$], 39.6 and 39.4 [OOCC(CH$_3$)$_3$], 27.5 and 27.3 [OOCC(CH$_3$)$_3$] ppm. ^{1}H liquid NMR in CDCl$_3$: δ = 1.16 and 1.15 ppm (2 s). TGA: 20–355 °C (8.5 wt.-% loss), 355–410 °C (32 wt.-% loss), 410–455 °C (32 wt.-% loss). Selected IR data: $\tilde{v}$ = 2964 (w), 2930 (w), 2871 (w), 1543 (m), 1510 (w), 1483 (m), 1458 (m), 1426 (s), 1414 (s), 1377 (s), 1360 (s), 1228 (m), 1033 (m), 938 (w), 896 (w), 783 (s), 736 (w), 602 (w)

cm^{-1}. C$_{10.3}$H$_{18.75}$N$_{0.25}$O$_5$Ti (384.2): calcd. C 45.6, H 6.8, N 1.3, Ti 17.3; found C 45.3, H 6.8, N 2.0, Ti 16.9.

Synthesis of Titanium–Oxo–Alkoxo–Carboxylate Species [TiO(OOCC$_6$H$_5$)$_{1.6}$(OiPr)$_{0.4}$]: Benzoic acid (2.148 g, 17.6 mmol) dissolved in acetonitrile (22 g, 536.6 mmol) was added dropwise to a solution of titanium(IV) isopropoxide (0.500 g, 1.76 mmol) in acetonitrile (2 g, 48.8 mmol) under argon. After a few minutes of stirring, the limpid solution was heated at 80 °C for 2 d and then cooled to 2 °C. After a few days, a fine white powder was recovered at the bottom of the flask. The solvent was then removed, the powder was washed with acetonitrile and finally dried under argon. This powder remained insoluble in most of the usual solvents. ^{13}C MAS solid-state NMR: δ = 175.8 and 172 (w, 11.1%, OOCC$_6$H$_5$ and HOOCC$_6$H$_5$), 130 (w, 56%, OOC$C$$_6H_5$), 86.30 [m, 2.6%, O$C$H(CH$_3$)$_2$], 24.47 [w, 4.5%, OCH($CH_3$)$_3$] ppm. Selected IR data (KBr pellets): $\tilde{v}$ = 3060 (w), 3030 (w), 2970 (w), 2890 (w), 1514 1692 (s), 1599 (s), 1514 (s), 1398 (s), 1130 (m), 1176 (m), 1010 (m), 716 (s), 672 (s), 488 (m) cm^{-1}. TGA: 20–250 °C (4.5 wt.-% loss), 250–390 °C (36 wt.-% loss), 390–480 °C (33.5 wt.-% loss). C$_{12.4}$H$_{10.8}$O$_{4.6}$Ti (281.2): calcd. C 52.9, H 3.8, Ti 17.1; found C 56.4, H 3.9, Ti 13.6.

Exchange of Molecules Trapped in the Ti$_8$Ph Cavity by Diethyl Ether, [Ti$_8$O$_8$(OOCC$_6$H$_5$)$_{16}$]·(C$_2$H$_5$OC$_2$H$_5$)$_2$·H$_2$O: Unground crystals of **Ti$_8$Ph** (0.331 g, 0.122 mmol) were dispersed in diethyl ether (14.1 g, 190 mmol) at room temperature. The dispersion was stirred at room temperature for 4 h. The yellow suspension obtained was then centrifuged and the resulting yellow powder dried by airflow at room temperature. C$_{15}$H$_{12.75}$O$_{5.38}$Ti (326.9): calcd. C 51.5, H 4.2, Ti 15.8; found C 50.4, H 4, Ti 15.7.

Synthesis of Titanium–Oxo–Carboxylate Cluster [Ti$_8$O$_8$-(OOCCH$_3$)$_{16}$]·(HOOCCH$_3$)$_2$ (Ti$_8$Me): A solution of Ti(OiPr)$_4$ (5.5 g, 19.3 mmol) and acetic acid (11.5 g, 192 mmol) in anhydrous acetonitrile (20.8 g, 507.8 mmol) was stirred at room temperature in a 50 mL Pyrex autoclave (transparent solution). The solution was heated at 100 °C for 60 h and cooled to room temperature. The white suspension was dispersed in acetonitrile (41.6 g, 1014 mmol) and filtered leading to a white powder (3.3 g, yield 95%) dried by airflow at room temperature. ^{13}C MAS solid-state NMR: δ = 184.5 and 182.7 (OOCCH$_3$), 23.4 and 22.7 (OOCCH_3) ppm. TGA: 20–270 °C (29 wt.-% loss), 270–305 °C (21.9 wt.-% loss), 305–350 °C (18.2 wt.-% loss). Selected IR data: $\tilde{v}$ = 3431 (w), 1756 (s), 1719 (s), 1703 (s), 1555 (m), 1457 (m), 1414 (s), 1348 (s), 1033 (s), 752 (w), 658 (m) cm^{-1}. C$_4$H$_6$O$_5$Ti (181.9): calcd. C 26.4, H 3.3, Ti 26.4; found C 25.7, H 3.6, Ti 27.1.

Synthesis of the Oxo Cluster [Ti$_8$O$_8$(OOCCH$_3$)$_{16}$] (Ti$_8$Me) from the Oxo Cluster [Ti$_8$O$_8$(OOCC$_6$H$_5$)$_{16}$] (Ti$_8$Ph): Unground crystals of **Ti$_8$Ph** (1.5 g, 0.554 mmol) were added to a solution of acetic acid (10.5 g, 174.7 mmol) and acetonitrile (78.6 g, 1914 mmol). The dispersion was stirred magnetically at reflux (80 °C) for 10 h and at room temperature for 12 h. The white suspension was centrifuged, and the resulting white solid dried by airflow at room temperature. The white powder was added afterwards to a second solution of acetic acid (10.5 g, 174.7 mmol) and acetonitrile (78.6 g, 1914 mmol). The dispersion was stirred magnetically at reflux (80 °C) for 10 h and at room temperature for 12 h. The white suspension was centrifuged and the resulting white solid dried by airflow at room temperature. Powder obtained from the first step corresponds to Ti$_8$O$_8$(C$_6$H$_5$COO)$_{2.5}$·(CH$_3$COOH)$_{13.5}$: found C 29.49, H 3.56, Ti 22.22. Powder obtained from the second step corresponds to Ti$_8$O$_8$(C$_6$H$_5$COO)$_1$·(CH$_3$COOH)$_{15}$: found C 26.0, H 3.8, Ti, 21.7.

Table 2. Crystal data, experimental, and refinement parameters for $[Ti_8O_8(OOCC_6H_5)_{16}]\cdot(CH_3CN)_2\cdot H_2O$ (**A**), $[Ti_8O_8(OOCC_6H_5)_{16}]\cdot(HOOCC_6H_5)_2\cdot H_2O$ (**A'**), and $[Ti_8O_8\{OOCC(CH_3)_3\}_{16}]\cdot(C_4H_8O)_2$ (**B**).

	A	**A'**	**B**
Empirical formula	$C_{116}H_{88}N_2O_{41}Ti_8$	$C_{126}H_{94}O_{45}Ti_8$	$C_{88}H_{160}O_{42}Ti_8$
M_r [g mol^{-1}]	2549.08	2707.18	2273.36
T [K]	150(2)	150(2)	200(2)
λ [Å]	0.71073	0.71073	0.71073
Crystal system	tetragonal	tetragonal	monoclinic
Space group	$P4/nnc$ (no. 126)	$P4/nnc$ (no. 126)	$P2_1/c$ (no. 14)
a [Å]	16.779(2)	16.842(5)	25.559(7)
b [Å]	16.779(3)	16.842(5)	17.542(5)
c [Å]	23.737(3)	23.728(5)	31.614(9)
α [°]	90	90	90
β [°]	90	90	109.553(12)
γ [°]	90	90	90
V [Å^3]	6682.7(14)	6731(3)	13357(6)
Z	2	2	4
$\rho_{calcd.}$ [g cm^{-3}]	1.267	1.336	1.130
Crystal size [mm]	$0.44 \times 0.11 \times 0.11$	$0.22 \times 0.13 \times 0.11$	$0.4 \times 0.3 \times 0.2$
$F(000)$	2604	2764	4800
μ(Mo-K_α) [mm^{-1}]	0.528	0.530	0.520
No. of reflections collected	50142	61123	86541
No. of unique reflections	4901	3768	24271
Index ranges	$-23 \leq h \leq 23$	$-21 \leq h \leq 21$	$-30 \leq h \leq 33$
	$-14 \leq k \leq 23$	$-21 \leq k \leq 21$	$-22 \leq k \leq 21$
	$-33 \leq l \leq 32$	$-30 \leq l \leq 25$	$-41 \leq l \leq 41$
θ range for data collection [°]	1.70–30.00	1.71–27.21	1.69–27.5
R_{int}	0.080	0.120	0.0538
Data/restraints/parameters	4901/57/248	3768/124/275	24271/5/1243
R_1 [$I > 2\sigma(I)$]	0.1035	0.1053	0.0811
wR_2 (all data)	0.2823	0.2470	0.3196
Goodness of fit on F^2	1.267	1.190	1.041
$\Delta\rho_{max/min}$ [e Å^{-3}]	1.03/–0.90	0.59/–0.55	1.340/–0.684

Synthesis of the Oxo Cluster $[Ti_8O_8\{OOC(CH_3)_3\}_{16}]$ (Ti$_8$*t*Bu) from the Oxo Cluster $[Ti_8O_8(OOCC_6H_5)_{16}]$ (Ti$_8$Ph): Ground crystals of Ti$_8$Ph (0.76 g, 0.28 mmol) were added to a solution of pivalic acid (5.6 g, 56 mmol) in xylene (25 g, 235 mmol). The yellow dispersion was stirred magnetically at reflux for 10 h. The dispersion was then cooled to room temperature for 12 h and then dried under vacuum at 120 °C. A white powder was obtained and washed in acetonitrile. The powder was dispersed twice in a solution of pivalic acid (5.6 g, 56 mmol) in acetonitrile (47 g, 1150 mmol). The dispersion was placed in a 100 mL Pyrex autoclave and heated at 100 °C over 3 d. A white powder was retrieved by filtration, dissolved in toluene and recrystallized at –17 °C. ^{13}C NMR in CDCl$_3$: δ = 189.2 and 187.7 [OO*C*C(CH$_3$)$_3$], 39.6 and 39.4 [OOC*C*(CH$_3$)$_3$], 27.5 and 27.3 [OOCC(*C*H$_3$)$_3$] ppm. ^{1}H NMR in CDCl$_3$: δ = 1.16 and 1.15 (2 s) ppm. TGA: 20–355 °C (8.5 wt.-% loss), 355–410 °C (32 wt.-% loss), 410–455 °C (32 wt.-% loss). Selected IR data: $\tilde{\nu}$ = 2964 (w), 2930 (w), 2871 (w), 1543 (m), 1510 (w), 1483 (m), 1458 (m), 1426(s), 1414(s), 1377(s), 1360(s), 1228(m), 1033 (m), 938(w), 896(w), 783(s), 736(w), 602 (w) cm^{-1}. $C_{10.3}H_{18.75}N_{0.25}O_5Ti$ (273.8): calcd. C 45.6, H 6.8, N 1.3, Ti 17.3, found C 45.3, H, 6.8, N 2.0, Ti 16.9.

Crystal Data: Data were recorded at 150 or 200 K with a Kappa-CCD Bruker diffractometer with graphite-monochromated Mo-K_α radiation (λ = 0.71073 Å) by using the ω-scan technique, and were corrected by empirical absorption corrections (SADABS). The structures were solved by direct methods and refined with full-matrix least-squares techniques using the SHELXS-97 and SHELXL-97 programs.[64] All non-hydrogen atoms were refined anisotropically. The crystallographic data are summarized in Table 2. CCDC-780782 (for **A**), -780783 (for **A'**), -780784 (for **B**) contain the supplementary crystallographic data for this paper. These data can be obtained free of charge from The Cambridge Crystallographic Data Centre via www.ccdc.cam.ac.uk/data_request/cif.

Supporting Information (see footnote on the first page of this article): Powder XRD patterns, IRTF spectrum, and ^{13}C MAS NMR spectrum of TiO(C$_6$H$_5$COO)$_{1.6}$(O*i*Pr)$_{0.4}$.

[1] P. Gomèz-Romero, C. Sanchez, *Functional Hybrid Materials*, Wiley-VCH, Verlag GmbH & Co. KGaA, **2004**.
[2] G. Kickelbick, *Hybrid Materials*, Wiley-VCH, Verlag GmbH & Co. KGaA, **2007**.
[3] C. Sanchez, F. Ribot, *New J. Chem.* **1994**, *18*, 1007.
[4] J. Livage, M. Henry, C. Sanchez, *Prog. Solid State Chem.* **1988**, *18*, 259.
[5] C. Sanchez, L. Rozes, F. Ribot, C. Laberty-Robert, D. Grosso, C. Sassoye, C. Boissiere, L. Nicole, *C. R. Chim.* **2010**, *13*, 3.
[6] C. Sanchez, B. Julian, P. Belleville, M. Popall, *J. Mater. Chem.* **2005**, *15*, 3559.
[7] C. Sanchez, B. Lebeau, F. Chaput, J. P. Boilot, *Adv. Mater.* **2003**, *15*, 1969.
[8] C. Sanchez, H. Arribart, M. M. G. Guille, *Nat. Mater.* **2005**, *4*, 277.

[9] C. Sanchez, C. Boissiere, D. Grosso, C. Laberty, L. Nicole, *Chem. Mater.* **2008**, *20*, 682.

[10] U. Schubert, *Chem. Mater.* **2001**, *13*, 3487.

[11] C. Sanchez, G. Soler-Illia, F. Ribot, T. Lalot, C. R. Mayer, V. Cabuil, *Chem. Mater.* **2001**, *13*, 3061.

[12] L. Rozes, N. Steunou, G. Fornasieri, C. Sanchez, *Monatsh. Chem.* **2006**, *137*, 501.

[13] F. Ribot, C. Sanchez, *Comments Inorg. Chem.* **1999**, *20*, 327.

[14] I. Gautier Luneau, A. Mosset, J. Galy, *Z. Kristallogr.* **1987**, *180*, 83.

[15] T. J. Boyle, T. M. Alam, C. J. Tafoya, B. L. Scott, *Inorg. Chem.* **1998**, *37*, 5588.

[16] V. W. Day, T. A. Eberspacher, W. G. Klemperer, C. W. Park, *J. Am. Chem. Soc.* **1993**, *115*, 8469.

[17] C. F. Campana, Y. Chen, V. W. Day, W. G. Klemperer, R. A. Sparks, *J. Chem. Soc., Dalton Trans.* **1996**, 691.

[18] V. W. Day, T. A. Eberspacher, Y. W. Chen, J. L. Hao, W. G. Klemperer, *Inorg. Chim. Acta* **1995**, *229*, 391.

[19] U. Schubert, E. Arpac, W. Glaubitt, A. Helmerich, C. Chau, *Chem. Mater.* **1992**, *4*, 291.

[20] B. Moraru, N. Husing, G. Kickelbick, U. Schubert, P. Fratzl, H. Peterlik, *Chem. Mater.* **2002**, *14*, 2732.

[21] I. Mijatovic, G. Kickelbick, U. Schubert, *Eur. J. Inorg. Chem.* **2001**, 1933.

[22] I. Mijatovic, G. Kickelbick, M. Puchberger, U. Schubert, *New J. Chem.* **2003**, *27*, 3.

[23] G. Kickelbick, U. Schubert, *Eur. J. Inorg. Chem.* **1998**, 159.

[24] Y. Gao, N. R. Choudhury, J. Matisons, U. Schubert, B. Moraru, *Chem. Mater.* **2002**, *14*, 4522.

[25] G. Kickelbick, D. Holzinger, C. Brick, G. Trimmel, E. Moons, *Chem. Mater.* **2002**, *14*, 4382.

[26] P. Toledano, M. In, C. Sanchez, *C. R. Acad. Sci., Ser. II* **1991**, *313*, 1247.

[27] S. Doeuff, Y. Dromzee, C. Sanchez, *C. R. Acad. Sci., Ser. II* **1989**, *308*, 1409.

[28] S. Doeuff, Y. Dromzee, F. Taulelle, C. Sanchez, *Inorg. Chem.* **1989**, *28*, 4439.

[29] N. Steunou, F. Robert, K. Boubekeur, F. Ribot, C. Sanchez, *Inorg. Chim. Acta* **1998**, *279*, 144.

[30] N. Steunou, F. Ribot, K. Boubekeur, J. Maquet, C. Sanchez, *New J. Chem.* **1999**, *23*, 1079.

[31] N. Steunou, G. Kickelbick, K. Boubekeur, C. M. Sanchez, *J. Chem. Soc., Dalton Trans.* **1999**, 3653.

[32] S. Le Calve, B. Alonso, L. Rozes, C. Sanchez, M. N. Rager, D. Massiot, *C. R. Chim.* **2004**, *7*, 241.

[33] G. Fornasieri, L. Rozes, S. Le Calve, B. Alonso, D. Massiot, M. N. Rager, M. Evain, K. Boubekeur, C. Sanchez, *J. Am. Chem. Soc.* **2005**, *127*, 4869.

[34] S. Bocchini, G. Fornasieri, L. Rozes, S. Trabelsi, J. Galy, N. E. Zafeiropoulos, M. Stamm, J. F. Gerard, C. Sanchez, *Chem. Commun.* **2005**, 2600.

[35] S. Trabelsi, G. Fornasieri, L. Rozes, A. Janke, A. Mensch, C. Sanchez, M. Stamm, *J. Appl. Crystallogr.* **2006**, *39*, 656.

[36] L. Rozes, G. Fornasieri, S. Trabelsi, C. Creton, N. E. Zafeiropoulos, M. Stamm, C. Sanchez, *Prog. Solid State Chem.* **2005**, *33*, 127.

[37] A. I. Kuznetsov, O. Kameneva, N. Bityurin, L. Rozes, C. Sanchez, A. Kanaev, *Phys. Chem. Chem. Phys.* **2009**, *11*, 1248.

[38] G. Soler-Illia, L. Rozes, M. K. Boggiano, C. Sanchez, C. O. Turrin, A. M. Caminade, J. P. Majoral, *Angew. Chem. Int. Ed.* **2000**, *39*, 4250.

[39] L. Rozes, S. Cochet, T. Frot, G. Fornasieri, C. Sassoye, M. Popall, C. Sanchez, *Organic/Inorganic Hybrid Materials 2007* (Eds.: C. Barbé, R. M. Laine, C. Sanchez, U. Schubert), *Mater. Res. Soc. Symp. Proc.*, Warrendale, PA, **2007**, vol. 1007, p. 241.

[40] S. Trabelsi, A. Janke, R. Hassler, N. E. Zafeiropoulos, G. Fornasieri, S. Bocchini, L. Rozes, M. Stamm, J. F. Gerard, C. Sanchez, *Macromolecules* **2005**, *38*, 6068.

[41] S. Doeuff, M. Henry, C. Sanchez, J. Livage, *J. Non-Cryst. Solids* **1987**, *89*, 206.

[42] U. Schubert, N. Husing, A. Lorenz, *Chem. Mater.* **1995**, *7*, 2010.

[43] U. Schubert, *J. Mater. Chem.* **2005**, *15*, 3701.

[44] S. Doeuff, M. Henry, C. Sanchez, *Mater. Res. Bull.* **1990**, *25*, 1519.

[45] M. Niederberger, G. Garnweitner, *Chem. Eur. J.* **2006**, *12*, 7282.

[46] M. Niederberger, *Acc. Chem. Res.* **2007**, *40*, 793.

[47] A. Pandey, V. D. Gupta, H. Noth, *Eur. J. Inorg. Chem.* **2000**, 1351.

[48] T. J. Boyle, R. P. Tyner, T. M. Alam, B. L. Scott, J. W. Ziller, B. G. Potter, *J. Am. Chem. Soc.* **1999**, *121*, 12104.

[49] P. I. Laaziz, A. Larbot, C. Guizard, J. Durand, L. Cot, J. Joffre, *Acta Crystallogr., Sect. C Cryst. Struct. Commun.* **1990**, *46*, 2332.

[50] X. J. Lei, M. Y. Shang, T. P. Fehlner, *Organometallics* **1996**, *15*, 3779.

[51] R. Ghosh, M. Nethaji, A. G. Samuelson, *Chem. Commun.* **2003**, 2556.

[52] H. Barrow, D. A. Brown, N. W. Alcock, H. J. Clase, M. G. H. Wallbridge, *J. Chem. Soc., Chem. Commun.* **1995**, 1231.

[53] P. Piszczek, M. Richert, A. Grodzicki, T. Glowiak, A. Wojtczak, *Polyhedron* **2005**, *24*, 663.

[54] K. A. Udachin, G. D. Enright, C. I. Ratcliffe, J. A. Ripmeester, *ChemPhysChem* **2003**, *4*, 1059.

[55] E. B. Brouwer, K. A. Udachin, G. D. Enright, C. I. Ratcliffe, J. A. Ripmeester, *Chem. Commun.* **1998**, 587.

[56] G. Ferey, *Chem. Soc. Rev.* **2008**, *37*, 191.

[57] D. Bradshaw, J. B. Claridge, E. J. Cussen, T. J. Prior, M. J. Rosseinsky, *Acc. Chem. Res.* **2005**, *38*, 273.

[58] S. Kitagawa, R. Kitaura, S. Noro, *Angew. Chem. Int. Ed.* **2004**, *43*, 2334.

[59] M. Dan-Hardi, C. Serre, T. Frot, L. Rozes, G. Maurin, C. Sanchez, G. Ferey, *J. Am. Chem. Soc.* **2009**, *131*, 10857.

[60] M. O'Keeffe, O. M. Yaghi, *J. Solid State Chem.* **2005**, *178*, V.

[61] A. J. Fletcher, K. M. Thomas, M. J. Rosseinsky, *J. Solid State Chem.* **2005**, *178*, 2491.

[62] J. L. C. Rowsell, O. M. Yaghi, *Angew. Chem. Int. Ed.* **2005**, *44*, 4670.

[63] J. L. C. Rowsell, A. R. Millward, K. S. Park, O. M. Yaghi, *J. Am. Chem. Soc.* **2004**, *126*, 5666.

[64] G. M. Sheldrick, *SHELXL, SHELXS, Programs for Crystal Structure Analysis*, University of Göttingen, Germany, **1997**.

[65] A. E. Bennett, C. M. Rienstra, M. Auger, K. V. Lakshmi, R. G. Griffin, *J. Chem. Phys.* **1995**, *103*, 6951.

[66] H. E. Gottlieb, V. Kotlyar, A. Nudelman, *J. Org. Chem.* **1997**, *62*, 7512.